Thermal transport in two- and three-dimensional nanowire networks

Maxime Verdier and David Lacroix
Université de Lorraine, LEMTA UMR 7563, 54505 Vandoeuvre les Nancy, France

Konstantinos Termentzidis*
Université Lyon, CNRS, INSA-Lyon, Université Claude Bernard Lyon 1, CETHIL UMR5008, F-69621, Villeurbanne, France and Université de Lorraine, LEMTA UMR 7563, 54505 Vandoeuvre les Nancy, France

(Received 16 February 2018; published 23 October 2018)

Two-dimensional (2D) and three-dimensional (3D) nanowire networks are potential metastructures for nanoelectronics and thermoelectric applications. This new class of nanoarchitectured materials have interesting physical properties due to their low mass density and their high surface-to-volume ratio. Here, we report on thermal transport properties in 2D and 3D interconnected nanowire networks. The thermal conductivity of these networks decreases in increasing the distance between the nodes. This effect is much more pronounced in 3D networks due to increased porosity, surface-to-volume ratio, and the enhanced backscattering at 3D nodes compared to 2D nodes. We propose a model to estimate the thermal resistance related to the 2D and 3D interconnections in order to provide an analytic description of thermal conductivity of such nanowire networks; the latter is in good agreement with molecular dynamic results. The backscattering processes in the nodes increase the thermal resistance by a factor of 5 compared to simple nanowires.

DOI: 10.1103/PhysRevB.98.155434

I. INTRODUCTION

New innovating and highly sophisticated architectured nanostructures are now feasible with the rapid evolution of the elaboration methods [1–4]. Among them two- and three-dimensional (2D, 3D) networks of nanowires are a new class of nanostructured materials with interesting mechanical, optical, electronic, and thermal properties. 2D networks are proposed as optoelectronic or biological devices and sensors due to their mechanical strength and flexibility [4]. Furthermore, 2D or 3D ordered or disordered networks could be useful for complex integrated nanoelectronic circuits [5]. Independently of their application, their main characteristics are the extremely low mass density, the high surface-to-volume ratio, as well as high porosity and their remarkable mechanical properties. In the literature, 3D networks have been elaborated during the last decade at the nanoscale with several different materials (silver [6], manganese dioxide [7], or silicon [8,9]).

There are three main fields of applications for silicon nanowire (NW) networks and nanomeshes. (i) Thermoelectricity (TE): The huge surface-to-volume ratio of such nanostructures reduces strongly their lattice thermal conductivity (TC), making Si NW networks promising candidates for TE applications [10–13]. (ii) Transistors: These systems can be easily integrated in nanoelectronic devices (Si compatible) and could be the next generation of transistors, thanks to their high density of nanowire interconnections [14–16]. (iii) Catalysis: Nanowire networks are interesting for catalysis applications because of their large surface-to-volume ratio that allows improved efficiency of chemical reactions. Furthermore, their strong mechanical robustness as compared to isolated nanowires or nanoparticles makes them interesting candidates to practically achieve all these innovative applications [1,17].

Concerning the thermal properties of nanostructures, they have attracted high attention for various applications in the fields of microelectronics, optoelectronics, and energy harvesting. Nanoscale heat transfer is known to diverge from classical physics [18], especially in semiconductors where heat is mostly carried by lattice vibrations (phonons). Interestingly, nanostructuration usually reduces the TC due to boundary scattering, while the electrical properties could be preserved [19]. The design of nanostructured materials with ultra-low TC, beating sometimes the amorphous limit while keeping a large crystalline fraction, is now possible [20,21]. Nanoporous materials may have even lower thermal conductivity because of the removal of material [22,23].

In this work, we focus on a specific architectured nanostructure which consists of interconnected silicon nanowires with a square cross section forming a 2D or 3D network. At the beginning of the decade, the 2D networks (or nanomeshes) have been studied mainly due to their low TC but also as nanostructures in which coherent effects might be observed [10,24], as in membranes with periodic cylindrical pores [25]. Contrarily to 2D networks, the thermal properties of 3D NW networks have been scarcely investigated. Ma *et al* studied 3D periodic and aperiodic networks with very small nanowire diameters (about 1 nm) and they observed a strong effect of phonon localization at the nanowire crossings [26]. Honarvar and Hussein showed a 2 orders of magnitude reduction of the thermal conductivity due to resonance hybridization in silicon membranes with pillars on it [27]. The degrees of freedom of the pillars allow resonant modes to appear, which strongly affect thermal transport. In our work, we study 2D

*Konstantinos.Termentzidis@insa-lyon.fr

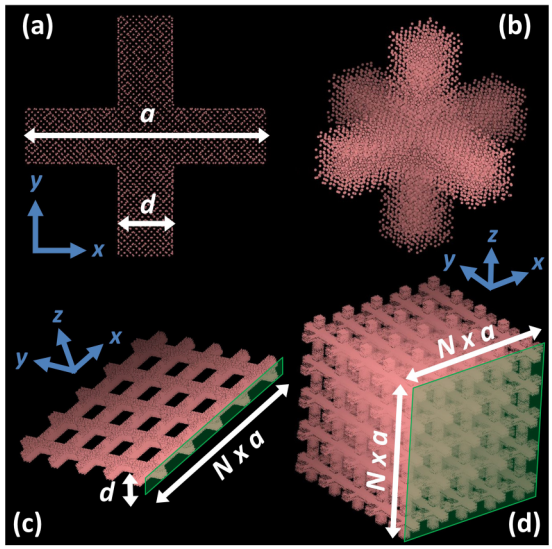

FIG. 1. Visualization of molecular dynamics systems of 2D and 3D nanowire networks. Simulation cell containing one node for (a) 2D and (b) 3D networks. (c), (d) Representation of global modeled systems thanks to periodic boundary conditions. The green surfaces represent the total cross section of each system when considering the TC in the direction perpendicular to these surfaces.

and 3D nanowire networks, which are quite different from the structures of Honarvar and Hussein. As the perpendicular branches connect with other nanowires, the networks are more robust and there are fewer degrees of freedom. This might prevent the formation of resonant modes in these structures.

Besides, two recent independent works [11,24] showed that thermal transport in nanomeshes is dominated by incoherent boundary scattering. Another novel study of heat transport in membranes with periodic cylindrical nanopores confirmed that coherent effects in silicon nanostructures are important only at low temperatures [28]. Moreover, we observed in precedent works [29,30] that the modifications of phonon density of states as compared to bulk ones are minor and weakly affect thermal transport in molecular dynamics simulations of nanostructures with sizes of some nanometers without amorphization. In this work, a systematic study of the heat-transport properties of nanowire networks, depending on their geometry and their dimensionality (2D or 3D), is conducted by means of molecular dynamics (MD) simulations. For the 2D networks, the TC is computed in the in-plane direction. The nanowires have a square cross section with dimensions $d \times d$ and they are interconnected with a 90° angle (Fig. 1).

The paper is organized as follows. First, the molecular dynamics simulation method is described. Then, thermal conductivities are given for periodic and isotropic networks. A model based on thermal resistance is derived and compared to the numerical results. Eventually, networks with different periods according to the direction are investigated. Conclusions are given at the end of the article.

II. SIMULATION DETAILS

All simulations were performed with LAMPPS open source software [31], using the Stillinger-Weber potential for silicon [32] with modified coefficients [33]. The structures are built from a slab of bulk crystalline silicon, deleting atoms of certain regions to obtain one "node" [Figs. 1(a) and 1(b)] of the nanowire's network. Periodic boundary conditions are applied along two or three directions to model an infinite 2D or 3D nanowire network, respectively [Figs. 1(c) and 1(d)]. Then a conjugate gradient minimization is done and the structures are relaxed at 300 K under *NVT* ensemble during 200 ps. Finally, the thermal conductivity at room temperature is extracted thanks to Green-Kubo formalism, estimating the correlation of flux fluctuations during 10 ns with a time window of 40 ps. To get the effective thermal conductivity, the volume in the Green-Kubo formula is taken as the total volume of the simulation box (including voids). Thus, it represents the heat flux able to flow through the total cross section of the structure. More computational details can be found in previous works [21,29]. Size effects due to the small size of the simulation box were checked, modeling a bigger structure containing four nodes of a 2D system. The difference between computed thermal conductivities with one and four nodes is less than 7% and remains within the error bars.

III. RESULTS AND DISCUSSION

A. Molecular dynamics results with isotropic networks

First, the effect of period a (the distance between two nodes centers) on thermal conduction is investigated. The cross section of the nanowires is set to 2.715×2.715 nm ($5\,a_0 \times 5\,a_0$). The effective TC κ of 2D and 3D nanowire networks is depicted in Fig. 2(a) as a function of the period. The TC decreases when the distance between nodes increases. This can be understood in terms of porosity (ϕ) and surface-to-volume ratio, which both increase upon increasing the period. Phonon boundary scattering occurs more often and thermal transport through the structure is hindered, especially for large periods. The reduction of TC as compared to the bulk (at 300 K, $\kappa_{bulk} \simeq 150\,\mathrm{W\,m^{-1}\,K^{-1}}$ with experimental measurements [34,35] and $\kappa_{bulk} \simeq 160\,\mathrm{W\,m^{-1}\,K^{-1}}$ with molecular dynamics) can reach 3 or 4 orders of magnitude in 2D and 3D networks, respectively. Such low values seem surprising but can be explained by the extremely high porosity, which reaches 81% for 2D networks and 97% for 3D networks studied here. Moreover, the S/V ratio is very large, and the phonon mean free path is drastically reduced [36,37]. All networks have a lower TC than a single nanowire of the same cross section $d \times d$, for which κ is found to be about $11\,\mathrm{W\,m^{-1}\,K^{-1}}$ with MD.

In order to distinguish the effects of porosity and nanostructuration on thermal transport, the thermal conductivity κ^* for an equivalent nonporous medium has been computed for the systems with $d = 2.715$ nm and different periods. The TC obtained with MD simulations can be written as

$$\kappa = \kappa_{bulk} f^* f(\phi), \tag{1}$$

with $f(\phi)$ the correction factor representing the reduction of the TC due to the porosity, and f^* the factor accounting for nanostructuration effects (phonon backscattering at free surfaces, coherent effects, etc.) that depend on several parameters, such as the S/V ratio. The equivalent TC is defined as $\kappa^* = \kappa_{bulk} f^*$. Thus, the effect of the porosity does not

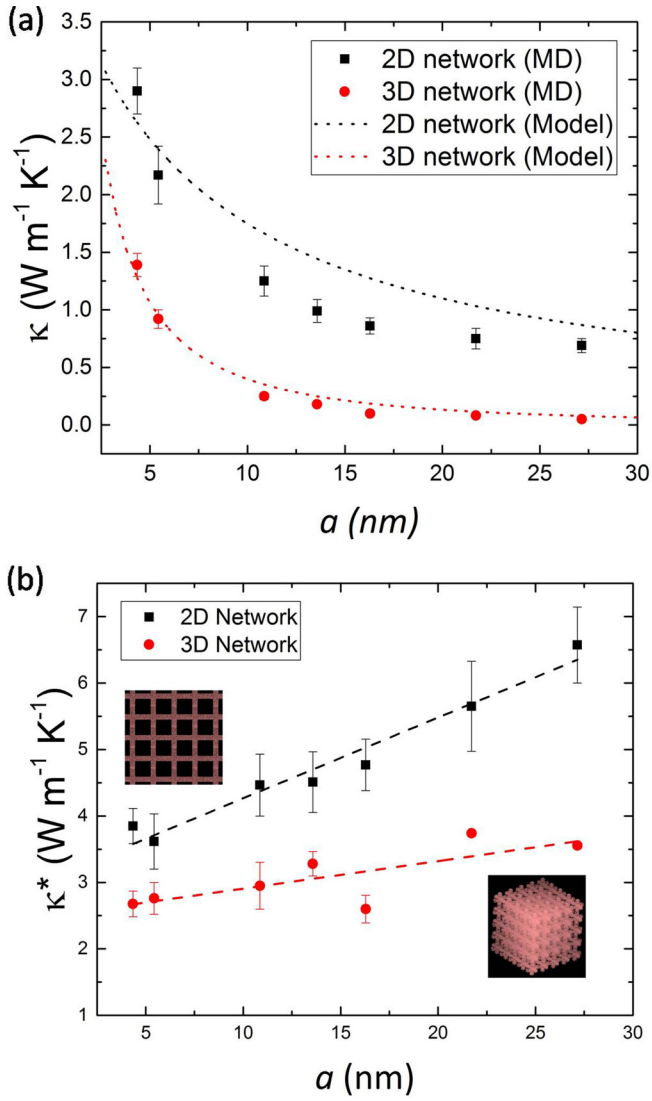

FIG. 2. Thermal conductivity of 2D and 3D nanowire networks as a function of period with a constant nanowire diameter $d = 2.715$ nm at room temperature. (a) Thermal conductivity κ obtained from EMD simulations, comparison with the thermal resistance model [Eqs. (8) and (9)]. (b) Thermal conductivity corresponding to an equivalent nonporous medium [$\kappa^* = \kappa(1+\phi)/(1-\phi)$].

appear in the equivalent TC and the reduction of κ^* is only due to the nanostructuration. In contrast with the effective thermal conductivity, it represents the heat flux able to flow through the cross section of the individual nanowires. $f(\phi)$ is taken from the Maxwell-Garnett effective medium model (EMM) [24]:

$$f(\phi) = (1-\phi)/(1+\phi). \tag{2}$$

Thus, the equivalent TC can be calculated from the value given by molecular dynamics with $\kappa^* = \kappa/f(\phi) = \kappa(1+\phi)/(1-\phi)$.

The equivalent TC goes from 3.8 to 6.6 W m^{-1} K^{-1} for 2D networks and 2.7 to 3.6 W m^{-1} K^{-1} for 3D networks as a goes from 4 to 27 nm [Fig. 2(b)], which seems reasonable given the huge S/V ratios. In contrast with the behavior of the effective TC κ, it is found for both 2D and 3D systems that

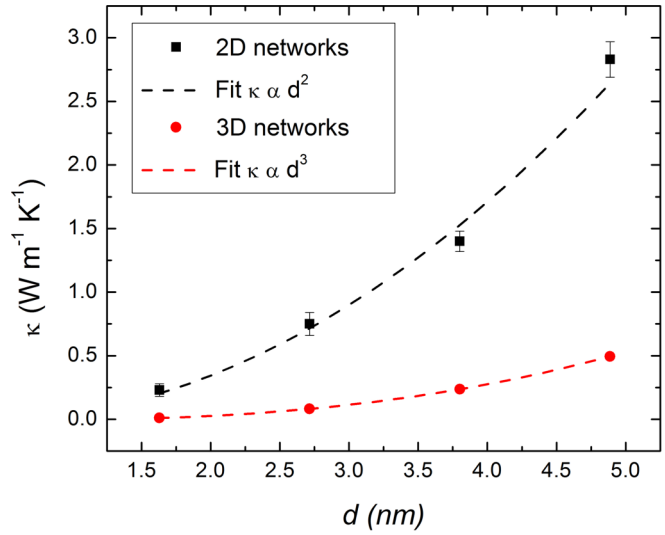

FIG. 3. Thermal conductivity of 2D and 3D nanowire networks as a function of nanowire diameter for a constant period $a = 21.72$ nm at $T = 300$ K.

κ^* slightly increases when the period increases, as expected from Refs. [24,26] due to less impact of backscattering at the nodes and possible phonon localization. Thus, the decrease of κ when increasing the period is mainly due to the growing porosity.

In spite of the increasing S/V ratio, which should lead to more phonon scattering, κ^* increases with the period. Similar observations have been done with 2D nanomeshes [24] and "fishbone" nanowires [38]. When considering one direction of measurement (direction of the heat flux), phonon scattering on the nanowires walls is not always resistive to heat transport. In nanowires parallel to the direction of interest, if scattering is fully diffuse, there is only 50% chance for each scattered phonon to go back (backscattering); while at the crossings with the perpendicular nanowires, which do not contribute to heat transport in the direction of measurement, phonons propagating along the heat flux direction and colliding with the walls are necessarily scattered backward. Moreover, it has been shown that free surfaces modeled in molecular dynamics have a great specularity, even at room temperature [30]. In the hypothetical case of fully specular walls, nanowires parallel to the heat flux are supposed not to be resistive at all, while perpendicular nanowires would lead to 100% of backscattering. Thus, the nodes hinder the TC more than the intrinsic thermal resistance of the nanowires. Increasing the period, the nodes move away from each other and there is less resistance to thermal transport, even if there is more scattering surface in the system. Thus, κ^* increases with the period. However, for very long periods, not considered here, the equivalent TC shall reach saturation to the TC of a single nanowire with cross section $d \times d$ ($\sim$11 W m^{-1} K^{-1}). For 3D networks, there are more phonon reflections at nodes than in 2D networks; this explains the lower κ^* in 3D networks.

The impact of the diameter of the nanowires on thermal transport has also been investigated. In Fig. 3 is depicted the TC κ of 2D and 3D nanowire networks with a constant period $a = 21.72$ nm as a function of the nanowire dimension d.

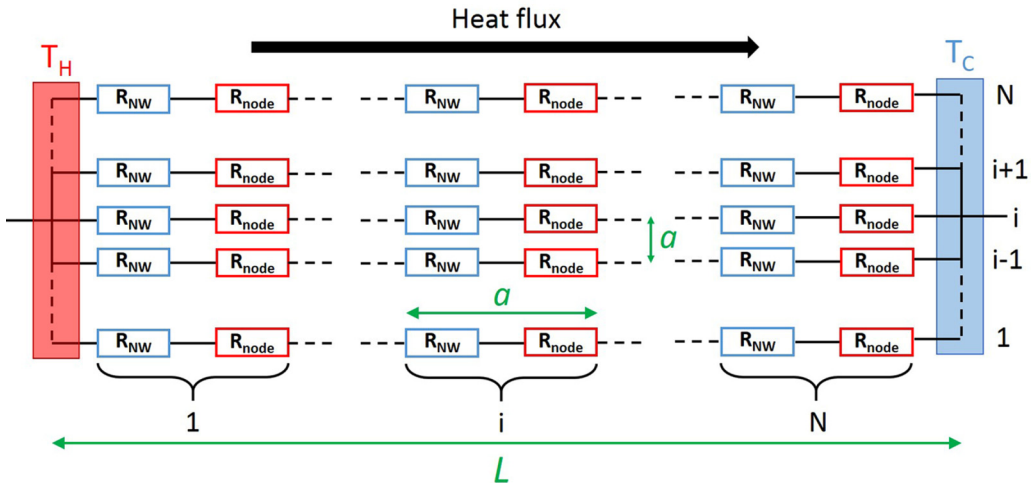

FIG. 4. Schematic of the thermal resistance model for a 2D nanowire network with $N \times N$ periods.

Obviously, by increasing the cross section of the nanowires, thermal transport is enhanced. Decreasing the diameter, the TC of 2D networks drops below $0.3\,\mathrm{W\,m^{-1}\,K^{-1}}$ while porosity varies from 60% to 85%. For 3D structures, κ is less than $1\,\mathrm{W\,m^{-1}\,K^{-1}}$ for all diameters, and the porosity is between 87% and 98%. For $d \simeq 5\,\mathrm{nm}$, the TC of the 3D network is divided by 300 as compared to the bulk. These dimensions can already be reached with current fabrication methods for MnO_2 nanowire networks [7]. Finally, we notice that the diameter-dependent TC of 2D networks increases with d^2, while 3D networks follow a d^3 law. This observation is valid when d is small compared to the period. When d tends toward a, the TC of 2D and 3D systems are expected to reach the values of a nanofilm of thickness d ($\kappa \simeq 23\,\mathrm{W\,m^{-1}\,K^{-1}}$) and of bulk silicon ($\kappa \simeq 160\,\mathrm{W\,m^{-1}\,K^{-1}}$), respectively.

Interestingly, heat conduction is always hindered further in a 3D network than in a 2D network, even for the same S/V ratio (TC as a function of S/V is plotted in the Supplemental Material [39]). For example, for $S/V \simeq 1.41\,\mathrm{nm^{-1}}$ the TC is about $0.8\,\mathrm{W\,m^{-1}\,K^{-1}}$ in 2D networks and less than $0.1\,\mathrm{W\,m^{-1}\,K^{-1}}$ in 3D networks). This observation is even valid when considering κ^* ($\kappa^*_{2D} \simeq 4.8\,\mathrm{W\,m^{-1}\,K^{-1}}$ and $\kappa^*_{3D} \simeq 3.7\,\mathrm{W\,m^{-1}\,K^{-1}}$ at the same $S/V \simeq 1.41\,\mathrm{nm^{-1}}$). This phenomenon is counterintuitive, as reduction of the dimensionality usually leads to lower TC.

B. Thermal resistances model

To explain the lower thermal transport in 3D structures, a model based on the use of thermal resistances has been developed. When a temperature gradient is applied within the network nanostructure, heat carriers are subject to two types of thermal resistances (Fig. 4). The first one is R_{NW}, the thermal resistance of a short nanowire ("strut") between two nodes (blue in Fig. 4), which depends on the cross section $d \times d$ and the length $a - d$ of each portion of nanowire [see Eq. (10)]. The second one is the thermal resistance related to the nodes R_{node} (red in Fig. 4), which is unknown. By analogy with macroscopic heat transfer, the heat flux per surface area J in the direction of the temperature gradient is given by Fourier's law,

$$J = -\kappa \frac{T_H - T_C}{L}, \tag{3}$$

with T_H and T_C the temperatures of hot and cold thermostats, respectively, and $L = N \times a$ the distance between the two thermostats (see Fig. 4). To reproduce the results of the present work, N has to tend toward infinity. Thus the model describes a cubic (or square) infinite nanowire network.

With respect to the thermal resistance formalism, the heat flux can also be written as

$$J = \frac{T_H - T_C}{R_{tot} S}, \tag{4}$$

where R_{tot} is the total thermal resistance and S is the total cross section (perpendicular to the flux) of the system. The total cross section of 2D networks is $S = Na \times d$, whereas for a 3D network $S = Na \times Na$ (see Fig. 1). From Eqs. (3) and (4), we derive the expression for thermal conductivity:

$$\kappa = \frac{L}{R_{tot} S}, \tag{5}$$

in which the total thermal resistance is different for 2D and 3D networks:

$$\frac{1}{R^{2D}_{tot}} = \frac{1}{R_{NW} + R^{2D}_{node}}, \tag{6}$$

$$\frac{1}{R^{3D}_{tot}} = \frac{N}{R_{NW} + R^{3D}_{node}}. \tag{7}$$

Combining the last three equations and replacing $L = Na$ and $S = Na \times d$ (2D) or $S = Na \times Na$ (3D), it comes to two simple expressions for thermal conductivity:

$$\kappa^{2D} = \frac{1}{d\left(R_{NW} + R^{2D}_{node}\right)}, \tag{8}$$

$$\kappa^{3D} = \frac{1}{a\left(R_{NW} + R^{3D}_{node}\right)}. \tag{9}$$

In order to determine R_{NW}, the thermal conductivity of an infinitely long nanowire with cross section $2.715 \times 2.715\,\mathrm{nm}$ has been computed with equilibrium molecular dynamics

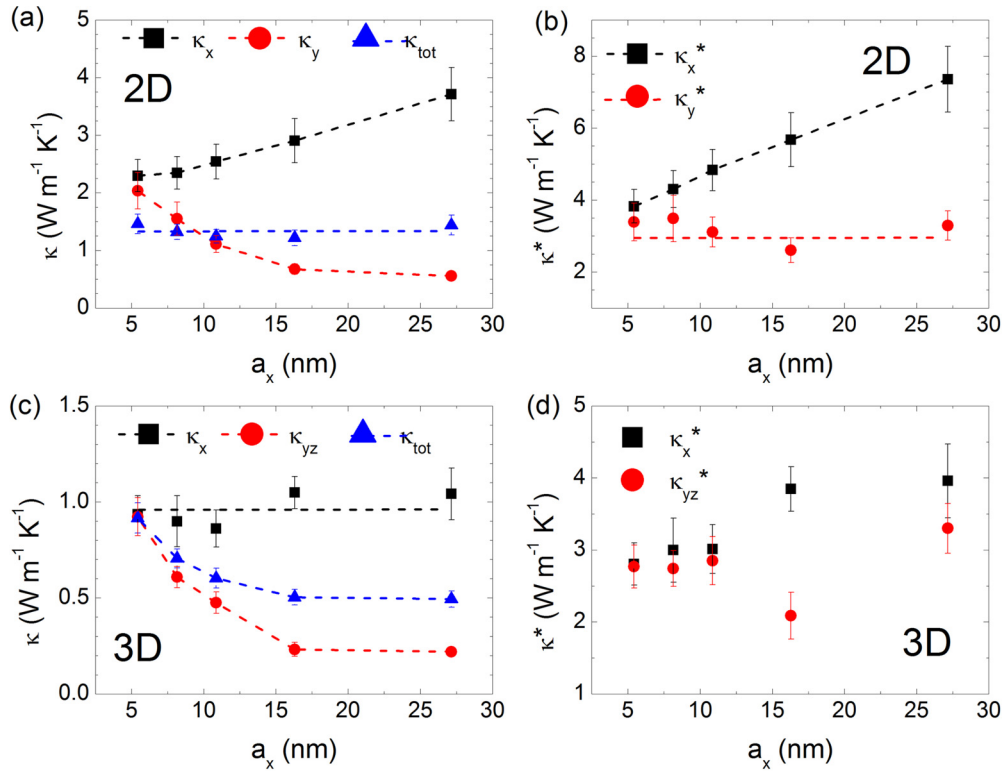

FIG. 5. Thermal conductivities of anisotropic nanowire networks. (a), (c) Thermal conductivity of 2D and 3D networks, respectively. (b), (d) Nonporous equivalent thermal conductivity of 2D and 3D networks, respectively.

(EMD). We obtained $\kappa_{NW} = 11 \pm 2\,\mathrm{W\,m^{-1}\,K^{-1}}$. Then the thermal resistance of the portion of nanowire between two nodes is deduced for each system with

$$R_{NW} = \frac{a-d}{\kappa_{NW} d^2}. \tag{10}$$

Finally, R_{node} is chosen as the adjustable parameter. It is considered as a constant parameter for a given d, but it is not the same for 2D and 3D networks because the number of interconnected nanowires at a node is different (4 and 6, respectively). Each node corresponds to an abrupt change of cross section of the material for a length d. This surely affects thermal transport, but in a manner which is unknown. The proposed model allows one to quantify the thermal resistance due to the nodes. A simpler model for macroscopic wires networks is also provided in the Supplemental Material, and it fails to describe thermal properties of the nanostructures.

In Fig. 2 the nanoscale model is compared to EMD results for 2D and 3D nanowire networks with constant size of nanowire $d = 2.715$ nm and varying period. The simulations and model are in a particularly good quantitative agreement for 3D networks. The model correctly reproduces the trend for both 2D and 3D networks and predicts that thermal conduction in 3D systems is always lower than in 2D systems. This phenomenon mainly comes from the difference in total cross sections of 2D and 3D networks, which leads to a factor a/d between κ^{2D} and κ^{3D} in the model, assuming that $R^{2D}_{node} \simeq R^{3D}_{node}$ [see Eqs. (8) and (9)]. This factor is approximately retrieved from EMD results.

The best fit was obtained with $R_{node} = 1.2 \times 10^8\,\mathrm{K\,W^{-1}}$ for the 2D network and $R_{node} = 1.6 \times 10^8\,\mathrm{K\,W^{-1}}$ for the 3D network. For the sake of comparison, R_{NW} varies from 0.2×10^8 to $3.0 \times 10^8\,\mathrm{K\,W^{-1}}$ as a goes from 4 to 27 nm. The thermal resistance of a node is roughly equivalent to a 15-nm portion of nanowire with $d = 2.715$ nm, whereas the length of a node is only d. The impact of the nodes on thermal conduction is huge and cannot be neglected. At each node, some phonons experience backscattering because of the free surface of perpendicular nanowires and this greatly reduces thermal transport [24,29]. Moreover, the node resistance is found to be slightly higher for 3D networks than 2D networks. This is related to the fact that 3D nodes have four perpendicular branches (compared to two perpendicular branches for 2D nodes), so more backscattering occurs at 3D nodes. This also confirms what has been claimed above, explaining why even κ^* is lower for 3D systems than for 2D ones: this is due to the more important scattering at 3D nodes.

We can qualitatively compare the node resistance of the 2D networks with experimental measurements from the literature. The "NM" structures of Yu *et al.* [10] can be considered as 2D nanowire networks with dimensions (cross section and period) 1 order of magnitude larger than the structures studied in this work. From the measured thermal conductivity of their structures and the thermal conductivity of isolated nanowires [40], it is found [with Eqs. (8) and (10)] that their node resistance is 1 order of magnitude smaller than ours, which is consistent with the difference in the dimensions (when the cross section increases, the probability of backscattering at the nodes decreases). Moreover, for a similar ratio a/d, the ratios R_{node}/R_{NW} given by both studies are close to each other.

C. Quasiperiodic nanowires networks

In order to highlight the effect of backscattering at the nodes, we now investigate thermal conductivity variations as we increase the period a_x in the x direction while keeping $a_y = 5.43$ nm for 2D systems and $a_y = a_z = 5.43$ nm for 3D ones. The diameter of the nanowire is still $d = 2.715$ nm. The thermal conductivity in the x direction κ_x of 2D networks increases with a_x, whereas κ_y decreases [Fig. 5(a)]. For a given cross section, when looking to the heat flux in y direction, increasing a_x means that there are less and less channels to carry heat. Oppositely, when looking to heat flux in x direction, the density of nanowires remains the same whatever the value of a_x. κ_x is thus solely increasing due to the lowering of the thermal resistance induced by nodes that are less numerous as a_x increases. Interestingly, the decrease of κ_y and the increase of κ_x balance out and κ_{tot} is roughly constant as a_x increases, despite the growing porosity and S/V ratio.

In Fig. 5(b) is depicted the nonporous equivalent thermal conductivity κ^* as a function of a_x for the same systems. When the period is different in x and y directions, we have to modify a bit the equation to get κ^* along each axis [24]:

$$\begin{aligned}\kappa_x^* &= \frac{1+\phi\times a_y/a_x}{1-\phi}\kappa \\ \kappa_y^* &= \frac{1+\phi\times a_x/a_y}{1-\phi}\kappa\end{aligned}. \tag{11}$$

The increase of κ_x^* is even more pronounced than that of κ_x, because the effect of porosity, which tends to lower the thermal conductivity when a_x increases, has been removed. Moreover, the reduction of κ_y is not visible anymore. As the system has been reduced to an equivalent nonporous material, the density of nanowires in y direction does not matter.

For 3D networks, the trends are less clear. The thermal conductivities along the y and z axes are the same because $a_y = a_z$. The thermal conductivity in the (Oyz) plane κ_{yz} decreases when a_x increases [Fig. 5(c)] because of the reduced density of nanowires in y and z directions, as observed in 2D systems. But κ_x does not significantly increase. This shows a competition between the effects of the porosity and the backscattering at the nodes. The total thermal conductivity is not constant anymore because thermal transport is lowered in two directions.

When considering κ_x^* [Fig. 5(d)], the increase of the thermal conductivity due to the backscattering is more visible, though it is not as clear as for 2D systems. Moreover, κ_{yz}^* is not really constant. In particular, the value for $a_x = 16.29$ nm is very low and shall be considered with caution. A similar behavior occurs in Fig. 5(b) for 2D networks when $a_x = 16.29$ nm and has also been observed for isotropic 3D networks at $a = 16.29$ nm [Fig. 2(b)]. This could be due to new resonant modes appearing for specific dimensions of nanowires networks, as observed for nanowires with pillars [41].

Concerning the anisotropy of thermal conductivities between x and y directions, it is the same for 2D and 3D networks and it reaches 80% for $a_x = 27.15$ nm.

IV. CONCLUSION

To conclude, we investigated thermal conduction in 2D and 3D networks of interconnected silicon nanowires and we showed that the TC is drastically reduced in such structures due to a combination of large porosity and increased backscattering at the nodes. The lowering of thermal transport is more pronounced in the 3D networks than in the 2D networks, because 3D structures have higher porosity and their nodes have more branches, which leads to increased backscattering and larger thermal resistance. A model based on equivalent thermal resistances reproduces the main trends of the MD results and confirms these interpretations. The small discrepancy between model and simulations could arise from correlations between resistances, or from new vibrating modes emerging for specific dimensions of the networks. When elaborating these structures, an amorphization and oxidation of the free surfaces can occur, leading to less specular surfaces and accentuating the thermal conductivity reduction. This should be investigated in further works.

ACKNOWLEDGMENT

Calculations were performed on the EXPLOR Mesocenter (University of Lorraine).

[1] M. Rauber, I. Alber, S. Müller, R. Neumann, O. Picht, C. Roth, A. Schökel, M. E. Toimil-Molares, and W. Ensinger, Highly-ordered supportless three-dimensional nanowire networks with tunable complexity and interwire connectivity for device integration, Nano Lett. **11**, 2304 (2011).

[2] Q. Li, F. Yun, Y. Li, W. Ding, and Y. Zhang, Fabrication and application of indium-tin-oxide nanowire networks by polystyrene-assisted growth, Sci. Rep. **7**, 1600 (2017).

[3] R. Galland, P. Leduc, C. Guérin, D. Peyrade, L. Blanchoin, and M. Théry, Fabrication of three-dimensional electrical connections by means of directed actin self-organization, Nat. Mater. **12**, 416 (2013).

[4] B. Han, Y. Huang, R. Li, Q. Peng, J. Luo, K. Pei, A. Herczynski, K. Kempa, Z. Ren, and J. Gao, Bio-inspired networks for optoelectronic applications, Nat. Commun. **5**, 5674 (2014).

[5] J. M. Romo-Herrera, M. Terrones, H. Terrones, S. Dag, and V. Meunier, Covalent 2d and 3d networks from 1d nanostructures: Designing new materials, Nano Lett. **7**, 570 (2007).

[6] A. R. Madaria, A. Kumar, F. N. Ishikawa, and C. Zhou, Uniform, highly conductive, and patterned transparent films of a percolating silver nanowire network on rigid and flexible substrates using a dry transfer technique, Nano Res. **3**, 564 (2010).

[7] H. Jiang, T. Zhao, J. Ma, C. Yan, and C. Li, Ultrafine manganese dioxide nanowire network for high-performance supercapacitors, Chem. Commun. **47**, 1264 (2011).

[8] E. Mulazimoglu, S. Coskun, M. Gunoven, B. Butun, E. Ozbay, R. Turan, and H. E. Unalan, Silicon nanowire network metal-semiconductor-metal photodetectors, Appl. Phys. Lett. **103**, 083114 (2013).

[9] S. Ge, K. Jiang, X. Lu, Y. Chen, R. Wang, and S. Fan, Orientation-controlled growth of single-crystal silicon-nanowire arrays, Adv. Mater. **17**, 56 (2005).

[10] J.-K. Yu, S. Mitrovic, D. Tham, J. Varghese, and J. R. Heath, Reduction of thermal conductivity in phononic nanomesh structures, Nat. Nanotechnol. **5**, 718 (2010).

[11] N. K. Ravichandran and A. J. Minnich, Coherent and incoherent thermal transport in nanomeshes, Phys. Rev. B **89**, 205432 (2014).

[12] A. I. Hochbaum, R. Chen, R. D. Delgado, W. Liang, E. C. Garnett, M. Najarian, A. Majumdar, and P. Yang, Enhanced thermoelectric performance of rough silicon nanowires, Nature (London) **451**, 163 (2008).

[13] A. I. Boukai, Y. Bunimovich, J. Tahir-Kheli, J.-K. Yu, W. A. Goddard III, and J. R. Heath, Silicon nanowires as efficient thermoelectric materials, Nature (London) **451**, 168 (2008).

[14] A. I. Hochbaum, R. Fan, R. He, and P. Yang, Controlled growth of Si nanowire arrays for device integration, Nano Lett. **5**, 457 (2005).

[15] K. Heo, E. Cho, J.-E. Yang, M.-H. Kim, M. Lee, B. Y. Lee, S. G. Kwon, M.-S. Lee, M.-H. Jo, H.-J. Choi, T. Hyeon, and S. Hong, Large-scale assembly of silicon nanowire network-based devices using conventional microfabrication facilities, Nano Lett. **8**, 4523 (2008).

[16] D. Wang, H. Luo, R. Kou, M. P. Gil, S. Xiao, V. O. Golub, Z. Yang, C. J. Brinker, and Y. Lu, A general route to macroscopic hierarchical 3D nanowire networks, Angew. Chem. Int. Ed. **43**, 6169 (2004).

[17] Z. Wei, G. Wehmeyer, C. Dames, and Y. Chen, Geometric tuning of thermal conductivity in three-dimensional anisotropic phononic crystals, Nanoscale **8**, 16612 (2016).

[18] D. G. Cahill, P. V. Braun, G. Chen, D. R. Clarke, S. Fan, K. E. Goodson, P. Keblinski, W. P. King, G. D. Mahan, A. Majumdar, H. J. Maris, S. R. Phillpot, E. Pop, and L. Shi, Nanoscale thermal transport, II. 2003–2012, Appl. Phys. Rev. **1**, 011305 (2014).

[19] J.-H. Lee, G. A. Galli, and J. C. Grossman, Nanoporous Si as an efficient thermoelectric material, Nano Lett. **8**, 3750 (2008).

[20] H. Mizuno, S. Mossa, and J.-L. Barrat, Beating the amorphous limit in thermal conductivity by superlattices design, Sci. Rep. **5**, 14116 (2015).

[21] M. Verdier, K. Termentzidis, and D. Lacroix, Crystalline-amorphous silicon nano-composites: Nano-pores and nano-inclusions impact on the thermal conductivity, J. Appl. Phys. **119**, 175104 (2016).

[22] R. Dettori, C. Melis, X. Cartoixà, R. Rurali, and L. Colombo, Model for thermal conductivity in nanoporous silicon from atomistic simulations, Phys. Rev. B **91**, 054305 (2015).

[23] X. Cartoixà, R. Dettori, C. Melis, L. Colombo, and R. Rurali, Thermal transport in porous Si nanowires from approach-to-equilibrium molecular dynamics calculations, Appl. Phys. Lett. **109**, 013107 (2016).

[24] J. Lee, W. Lee, G. Wehmeyer, S. Dhuey, D. L. Olynick, S. Cabrini, C. Dames, J. J. Urban, and P. Yang, Investigation of phonon coherence and backscattering using silicon nanomeshes, Nat. Commun. **8**, 14054 (2017).

[25] P. E. Hopkins, C. M. Reinke, M. F. Su, R. H. Olsson, E. A. Shaner, Z. C. Leseman, J. R. Serrano, L. M. Phinney, and I. El-Kady, Reduction in the thermal conductivity of single crystalline silicon by phononic crystal patterning, Nano Lett. **11**, 107 (2011).

[26] D. Ma, H. Ding, H. Meng, L. Feng, Y. Wu, J. Shiomi, and N. Yang, Nano-cross-junction effect on phonon transport in silicon nanowire cages, Phys. Rev. B **94**, 165434 (2016).

[27] H. Honarvar and M. I. Hussein, Two orders of magnitude reduction in silicon membrane thermal conductivity by resonance hybridizations, Phys. Rev. B **97**, 195413 (2018).

[28] J. Maire, R. Anufriev, R. Yanagisawa, A. Ramiere, S. Volz, and M. Nomura, Heat conduction tuning by wave nature of phonons, Sci. Adv. **3**, e1700027 (2017).

[29] M. Verdier, D. Lacroix, and K. Termentzidis, Heat transport in phononic-like membranes: Modeling and comparison with modulated nano-wires, Int. J. Heat Mass Transf. **114**, 550 (2017).

[30] M. Verdier, D. Lacroix, S. Didenko, J.-F. Robillard, E. Lampin, T.-M. Bah, and K. Termentzidis, Influence of amorphous layers on the thermal conductivity of phononic crystals, Phys. Rev. B **97**, 115435 (2018).

[31] S. Plimpton, Fast parallel algorithms for short-range molecular dynamics, J. Comput. Phys. **117**, 1 (1995).

[32] F. H. Stillinger and T. A. Weber, Computer simulation of local order in condensed phases of silicon, Phys. Rev. B **31**, 5262 (1985).

[33] R. L. C. Vink, G. T. Barkema, W. F. van der Weg, and N. Mousseau, Fitting the Stillinger–Weber potential to amorphous silicon, J. Non-Cryst. Solids **282**, 248 (2001).

[34] C. J. Glassbrenner and G. A. Slack, Thermal conductivity of silicon and germanium from 3 K to the melting point, Phys. Rev. **134**, A1058 (1964).

[35] P. D. Maycock, Thermal conductivity of silicon, germanium, III-V compounds, and III-V alloys, Solid-State Electron. **10**, 161 (1967).

[36] A. Jain, Y.-J. Yu, and A. J. H. McGaughey, Phonon transport in periodic silicon nanoporous films with feature sizes greater than 100 nm, Phys. Rev. B **87**, 195301 (2013).

[37] V. Jean, S. Fumeron, K. Termentzidis, S. Tutashkonko, and D. Lacroix, Monte Carlo simulations of phonon transport in nanoporous silicon and germanium, J. Appl. Phys. **115**, 024304 (2014).

[38] J. Maire, R. Anufriev, T. Hori, J. Shiomi, S. Volz, and M. Nomura, Thermal conductivity reduction in silicon fishbone nanowires, Sci. Rep. **8**, 4452 (2018).

[39] See Supplemental Material at http://link.aps.org/supplemental/10.1103/PhysRevB.98.155434 for (i) thermal conductivity as a function of the surface-to-volume ratio and (ii) comparison with a macroscopic model.

[40] D. Lacroix, K. Joulain, D. Terris, and D. Lemonnier, Monte Carlo simulation of phonon confinement in silicon nanostructures: Application to the determination of the thermal conductivity of silicon nanowires, Appl. Phys. Lett. **89**, 103104 (2006).

[41] S. Xiong, K. Sääskilahti, Y. A. Kosevich, H. Han, D. Donadio, and S. Volz, Blocking Phonon Transport by Structural Resonances in Alloy-Based Nanophononic Metamaterials Leads to Ultralow Thermal Conductivity, Phys. Rev. Lett. **117**, 025503 (2016).